Multicolored Carbon Nanotubes: Decorating Patterned Carbon Nanotube Microstructures with Quantum Dots

Xiaodai Lim,[†] Yanwu Zhu,[†] Fook Chiong Cheong,[†] Nurmawati Muhammad Hanafiah,[§] Suresh Valiyaveettil,[§,‡] and Chorng-Haur Sow[†,‡,*]

[†]Department of Physics, Blk S12, Faculty of Science, National University of Singapore, 2 Science Drive 3, Singapore 117542, Singapore, [‡]Department of Chemistry, Faculty of Science, National University of Singapore, 3 Science Drive 3, Singapore 117543, Singapore, and [§]National University of Singapore Nanoscience and Nanotechnology Initiative, 2 Science Drive 3, Singapore 117542, Singapore

ABSTRACT In this work, techniques to create patterned array of multiwalled nanotube (MWNT) microstructures decorated with quantum dots (QDs) were presented. Using aligned array of intertwined MWNTs as the supporting template, a droplet of solution comprising QDs was deposited onto the MWNTs. When the solution evaporated away, QDs were left behind on the MWNT template. Coupled with the technique of laser pruning, a wide variety of QDs-decorated MWNT microstructures were created. In addition, the aligned array of MWNTs was found to be an effective nanosieve that could effectively sort out QDs with a size difference of ~0.5 nm. In this case, a droplet of solution comprising QDs of different sizes was placed on aligned array of MWNTs. As the solution spread across as well as trickled down the MWNTs, the smaller QDs were found to venture further and deeper into the MWNTs. Again coupled with laser pruning, fluorescence microscopy revealed multicolored MWNT microstructures due to preferential decoration of these QDs with difference sizes. As a result, multicolored/multicomponents hybrid functional materials were achieved.

KEYWORDS: carbon nanotubes · quantum dots · self-assembly · micropattern · nanosieve

Carbon nanotubes (CNTs) are fascinating nanomaterials with unique mechanical, electrical, and optical properties.[1–6] Suitable for a wide variety of applications, their versatility is truly remarkable. Since its discovery by Iijima,[1] CNTs have continued to captivate researchers. In recent years, great progress has been made in the synthesis and application studies of hybrid nanomaterial systems. One example of a hybrid system includes a controlled assembly of various nanomaterials onto CNTs template. There have been continuous efforts on novel studies involving alteration of physical properties of CNTs *via* the use of organic,[7] inorganic,[8] and biological species[9,10] to produce functionalized CNTs for further applications.[11] For example, Zhu *et al.*[12] fabricated CNTs beaded with ZnO nanoparticles by the simple heating of Zn-coated CNT. The hybrid nanomaterial exhibits tunable nonlinear optical absorption. Among these modifications, interactions between CNTs and semiconducting nanoparticles such as quantum dots (QDs) appear to be a well-matched and exciting combination in changing both optical[7] and electronic properties[13] of CNTs.

QDs possess size tunable optical and electronic properties resulting from quantum confinement.[14] Such properties allow them to be suitable candidates for applications in solar cells[15] and light emitting devices.[16] Having a high resistance to photobleaching, QDs are attractive materials for optoelectronics[17] and *in vivo* biosensing.[18,19] The technique of assembling QDs onto CNTs has drawn great attention. Ravindran *et al.*[20] were able to assemble CdSe/ZnS nanoparticles onto both ends of CNTs *via* a 1-ethyl-3(3-dimethylaminopropyl) carbodiimide HCl (EDC) reaction. The process coupled the carboxyl group in the CNTs to the amine group on the QDs produced through reacting methanol cleaned QDs suspended in toluene with 2-aminoethane thiol (AET) to form an amide linkage. These QDs-CNT-QDs heterostructures show great potential in electronic device applications. Robel *et al.*[15] made use of tetraoctylammonium bromide (TOAB) as a linker to secure CdS nanocrystallites on CNTs which exhibited the ability to respond to visible light and could be utilized in light-harvesting and optoelectronics applications. Having a possible potential of using such QDs/CNTs junctions on nanochips for future devices, it is thus highly desirable to achieve a simple and cost-effective technique to assemble QDs onto CNT microstructures on a large-scale basis.

An extension of these studies involves further developing of techniques to achieve assembly of these nanoparticles onto pat-

*Address correspondence to physowch@nus.edu.sg.

Received for review February 17, 2008 and accepted May 27, 2008.

Published online June 11, 2008.
10.1021/nn800101f CCC: $40.75

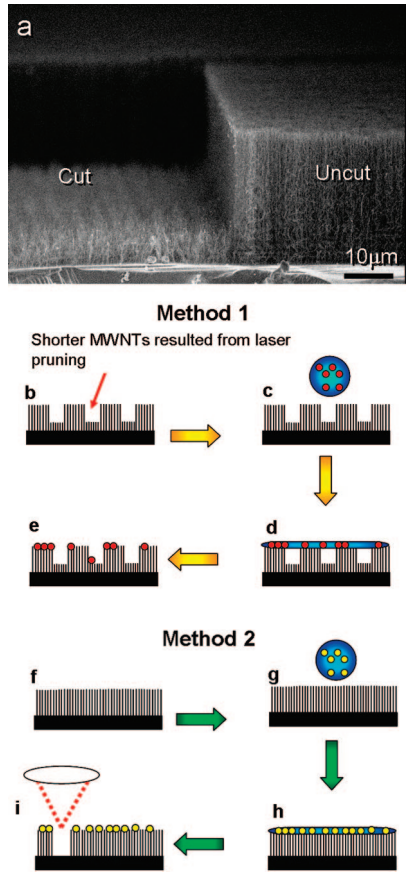

Figure 1. Schematic diagram of techniques used in assembling QDs onto patterned MWNTs. (a) SEM image of aligned array of MWNT sample with structures defined by laser pruning. Method 1: (b) Laser pruned channels on as-grown MWNTs. (c) Droplet of chloroform/toluene containing QDs was deposited onto the patterned sample. (d) The solution was left to dry in ambient conditions. (e) Once the solution had completely evaporated, QDs were left on the untrimmed regions of the sample. Method 2: (f) As-grown MWNTs. (g) Droplet of chloroform/toluene containing QDs was deposited onto the sample. (h) Spreading of QDs in solvent over sample. (i) Laser pruning of QD-covered sample.

terned and aligned array of CNT-based architectures en route to functional hybrid materials. For example, the CNTs array could serve as template for lining up QDs in a single row for applications within integral components of optical and electronic devices.[21] Upon assembly, collective physical properties of these QDs exhibit unique characteristics.[11] In such experiments, it is important to develop good control over selective assembly of QDs onto the micropatterns made of CNTs. One may start with QDs in aqueous suspension and deposit a droplet of the solution onto a patterned CNT. After evaporation, the QDs are left behind on the patterned CNT microstructures that act as supporting scaffolds. One of the challenging issues of this technique is the disruptive formation of cellular patterns due to influence of capillary forces during the drying process of solution from the CNTs surface as reported by Ajayan and Kane

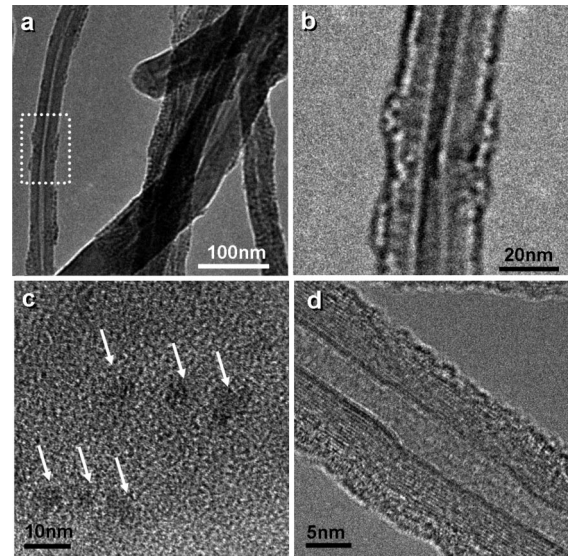

Figure 2. TEM images of (a) MWNTs decorated with QDs; (b) closed-up view of dotted rectangular box shown in panel a. HRTEM images of (c) CdSe/ZnS QDs supported by carbon film on standard TEM grid and (d) as-grown MWNT.

et al.[22] Hence, a method is necessary to overcome this problem and maintain the structures created. Moreover, it would be ideal to selectively assemble QDs according to their sizes onto CNTs during the self-assembly process. To the best of our knowledge, there has been no report on such a technique with high definition of QDs size-selective assembly. This could be attributed to the difficulty in sorting QDs differing in size by only a few nanometers.

In this work, we introduce a three-dimensional (3D) QDs and MWNT hybrid system created with a simple yet efficient technique. This involves depositing QDs in suspension onto laser patterned[23] MWNT microstructures. Using the laser pruning technique, not only did we overcome pattern distortion due to solvents containing QDs, we also demonstrated the creation of a

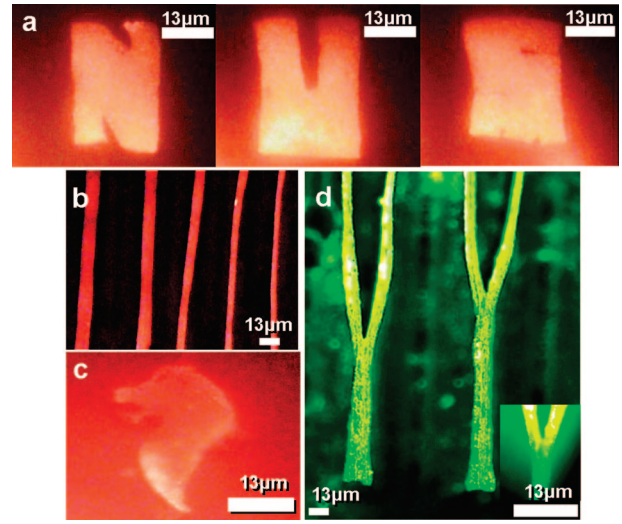

Figure 3. FM images of CdSe/ZnS QDs assembled onto patterned MWNTs using method 1: (a) "NUS", (b) simple channels, (c) Merlion, and (d) Y-junctions (inset: closed up view of the Y-junction).

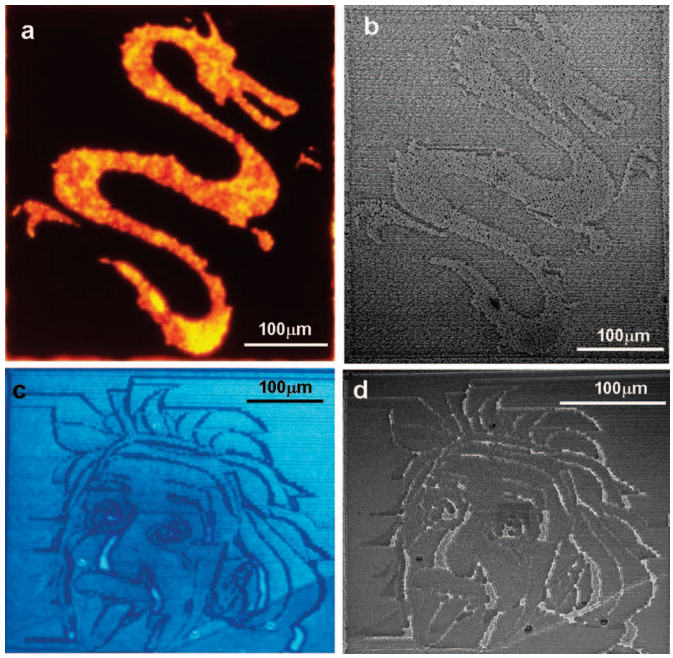

Figure 4. FM images of QDs decorated on patterned MWNTs obtained using method 2: (a) "Dragon" and (c) "Einstein". SEM images of same patterns: (b) "Dragon" and (d) "Einstein".

multicolored/multicomponent hybrid functional material through careful control of the laser power. In addition to the above, the ability of MWNTs to sort QDs with mere size difference of ~0.5 nm was also discovered.

RESULTS AND DISCUSSION

Introducing Methods of Assembling Particles onto MWNT Templates. To assemble particles onto desired regions of MWNT samples created *via* laser pruning as shown in Figure 1a, two methods were utilized in this work. Method 1: As shown in Figure 1b−e, QD-covered MWNT templates were left to dry in ambient conditions. After the solvent evaporated, QDs were found to assemble on the taller and untrimmed regions of the MWNT samples. Method 2: As seen in Figure 1f−i, QDs were first deposited onto the samples and left to dry in ambient conditions before undergoing laser pruning to create any desired structures. This technique was proven efficient in overcoming the problem of pattern distortions during drying. In addition, QDs were destroyed by heat generated from interactions between laser and MWNTs.

Interaction between Chloroform/Toluene with MWNTs. For a successful assembly process, we need to understand the interactions between chloroform/toluene with MWNTs. When a droplet of chloroform was deposited onto as grown MWNTs, the chloroform rapidly spreads across the as-grown MWNTs. Both toluene and chloroform exhibited similar behaviors upon interaction with MWNT surfaces. The difference lies in chloroform evaporating at a relatively faster rate than toluene. Other than this minor difference, the assembling of QDs in either solvent onto MWNTs achieved similar results. Hence, no specific distinctions between uses of these two solvents would be mentioned in our following discussions.

TEM Analysis of QDs Assembly on MWNTs. To study how QDs assemble onto MWNTs, TEM study was employed to investigate on the connections between them. Figure 2a shows a low-resolution TEM image of MWNTs after QDs had been deposited *via* method 1. A significant amount of QDs were seen to have attached onto the walls of MWNTs. Figure 2b shows a larger magnification of the region marked by the dotted rectangle in Figure 2a. As marked with the arrows, QDs with size of ~4.0 nm were observed on the MWNTs. Such observation is consistent with the

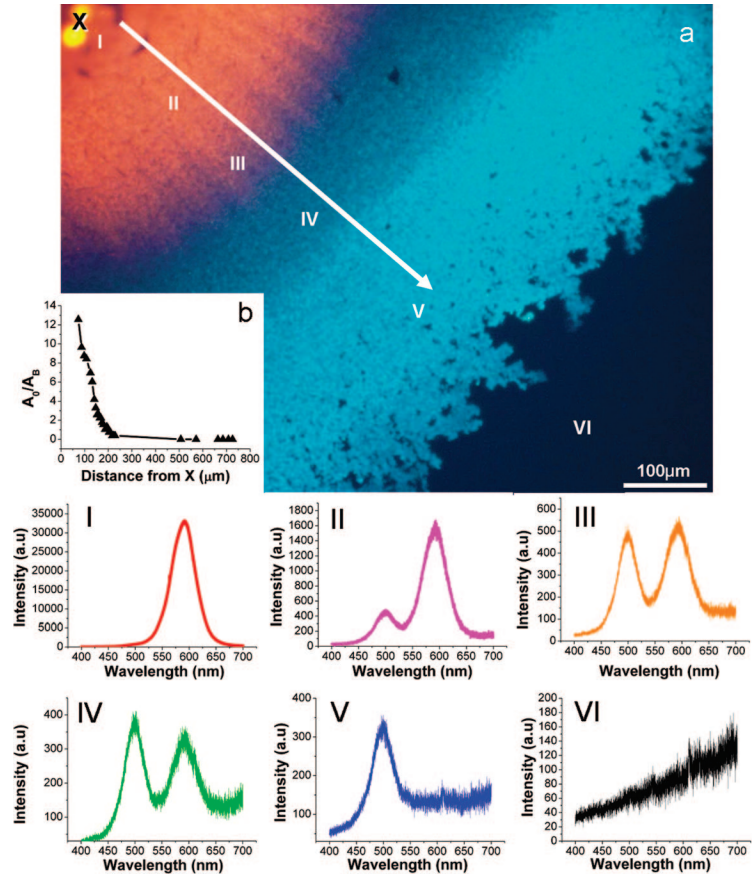

Figure 5. (a) FM images of sample created after depositing a droplet of QDs mixture. Orange QDs were observed to occupy the central region of the droplet as blue QDs spread out to a larger circumference in the lateral direction. PL spectra of (I) region I, (II) region II, (III) region III, (IV) region IV, (V) region V, and (VI) region VI reveal the types of QDs at each region. (b) Graph corresponding to ratio of area under orange peak to that of blue peak (A_O/A_B) with respect to distance from the point of reference X as indicated by the arrow in panel a.

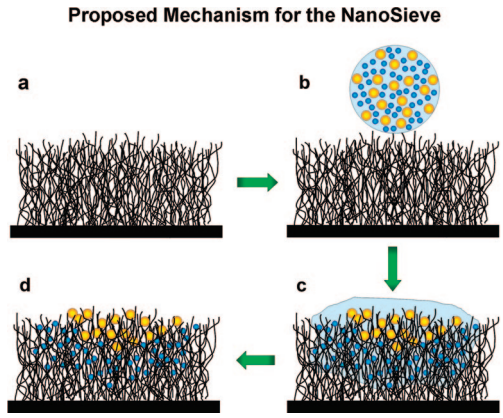

Figure 6. Proposed working mechanism of the 3D nanosieve. (a) Using as-grown MWNTs as the sorting medium, (b) a droplet of CdSe/ZnS QDs mixture with size difference of ~2.0 nm was introduced to the MWNT sample. (c) As the solvent spreads out, larger particles were first trapped because of the lack of mobility while smaller-sized particles were able to travel further and deeper into the MWNT network. (d) Finally, once the solvent had completely evaporated, CdSe/ZnS QDs remained attached onto MWNT sample.

TEM image of pure QDs as indicated by white arrows shown in Figure 2c. These QDs were supported by carbon film on a standard TEM grid. They were seen without distinct boundaries, and they did not appear to have prefect spherical shape. A strand of MWNT without any QDs attached to the surface was also taken for comparison purpose as shown in Figure 2d. In a comparison of the image in Figure 2d to that shown in Figure 2b, irregular attachments of QDs onto MWNT surfaces could be observed.

Comparison Between Assembly Method 1 and Method 2. Using method 1, different structures of MWNT with different fluorescent colors under fluorescence microscopy (FM) were created. Figure 3 shows orange QDs decorated (a) "NUS" letters formation, (b) channels, and (c) "Merlion". Changing size and hence color of the QDs, "Y-shaped" MWNT bundles with yellow illumination as seen in Figure 3d were created. In this case, parallel channels with width of 7.0 μm were observed to bundle together because of the influence of the capillary force during the evaporation of solvent. As the solvent dried before the strips bundled together completely,

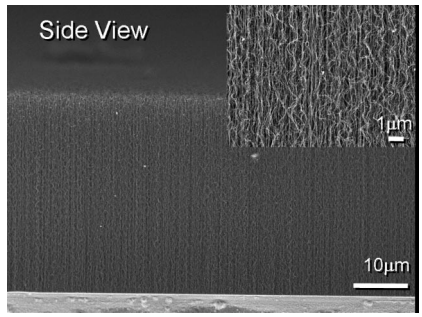

Figure 7. SEM image showing side view profile of the entangled MWNT array. Inset shows the SEM image of the same sample at a higher magnification.

Y-shaped MWNT bundles were formed. Despite using solvents that evaporated rapidly, pattern distortions during the drying process were still inevitable. On the other hand, method 2 was able to solve the problem of pattern distortion since structures were only created following QD-deposition on MWNTs. Damages to these QDs upon interaction with focused laser beam prevented them from emitting light upon excitation. As a result, structures created were not only visible under optical microscope/SEM due to structural differences but also visible under FM. The use of method 2 showed flexibility in creating patterns of different shapes and sizes. As shown in Figure 4, complicated images, such as "Dragon" and "Einstein", were created.

To show differences between methods 1 and 2, two similar patterns were created before and after deposition of QDs onto MWNTs, and the results were shown in Supporting Information, Figure S1. Figure S1a shows an SEM image of the original Merlion pattern pruned onto as-grown MWNTs. Figure S1b shows a FM image taken of the Merlion pattern created using method 1. Comparing Figure S1a to S1b, significant distortion to the Merlion pattern as a result of capillary force could be observed. Figure S1c shows a similar Merlion structure being created using method 2 with minimal distortion. Evidently, method 2 proved to be efficient in preventing pattern distortion caused by capillary force.

Lateral Nanosieve. For better controllability of the QDs assembly onto MWNTs, different sizes of quantum dots were used. These QDs of different sizes, 1.9 nm (blue emitting) and 4.0 nm (orange emitting), were mixed together with volume (nmol/mL) ratio of 7:1 in a small cylindrical bottle for ~2.0 min before a droplet of the mixture was extracted and deposited onto the MWNTs in a similar manner to method 2.

By depositing ~2.0 μL of QDs mixture onto the MWNTs, one would expect to see a mixture of blue and orange QDs covering top surface of the MWNT template similar to using single-sized QDs. However, from visual observation through the FM (Figure 5), distinctive orange and blue regions could be observed with a slightly darker blue shade that marks the interface of these two regions. Photoluminescence (PL) microscopy with same laser power was subsequently used to obtain a more quantitative measurement of light emitted from different regions on the decorated sample. The regions were labeled as shown in Figure 5a. Region I shows only a single PL peak, 592.2 ± 0.1 nm (Figure 5I). This peak formed in the wavelength range of orange visible light clearly corresponded to our visual observation. Moving outward into region II, a new peak appeared in the blue visible light range of the PL spectrum at 500.7 ± 0.1 nm together with the original peak at 593.0 ± 0.1 nm (Figure 5II). At the interface between the orange and the blue regions (region III), two PL peaks were identified (Figure 5III) at 498.7 ± 0.1 and

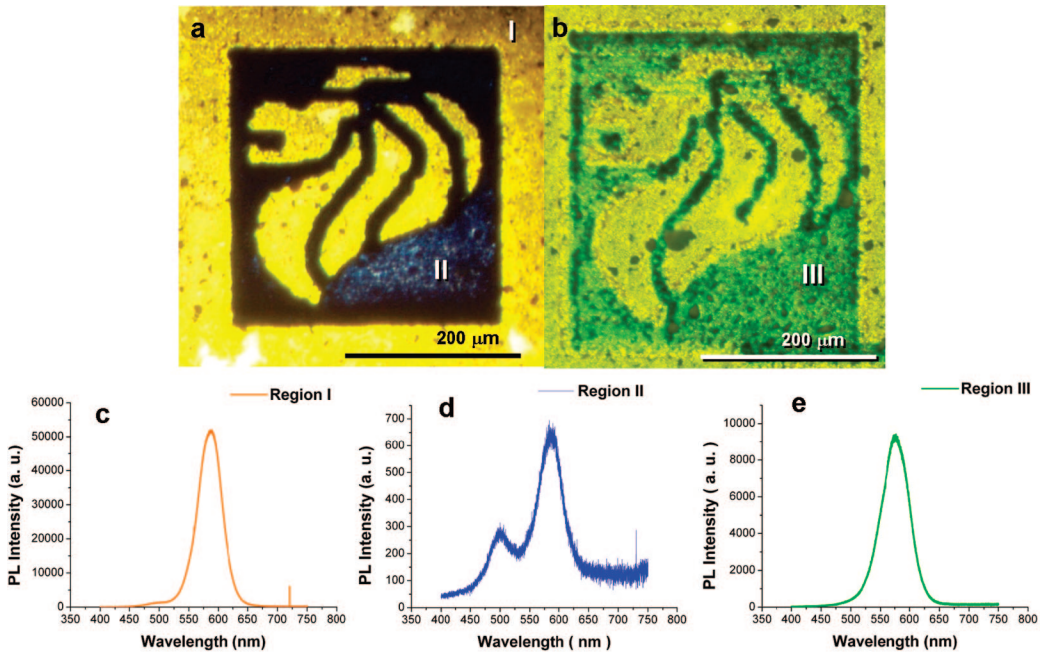

Figure 8. FM images (a and b) of laser pruned Merlion pattern produced using laser power of (a) ~40 mW with a depth of 7 μm and (b) ~23 mW with a depth of 1 μm. PL spectrums of (c) orange background, (d) blue, and (e) green trimmed regions indicated by I, II, and III, revealing the types of QDs at each region.

595.1 ± 0.1 nm, respectively, with intensity of the latter being slightly higher. Moving into region IV, while peaks at 502.2 ± 0.1 and 593.5 ± 0.1 nm (Figure 5IV) were still observed, what was considered more interesting was the interchange of peak intensities as compared to Figure 5III. In Figure 5IV, the peak in blue visible light range generated a slightly higher intensity than that in the orange visible light range. This result implied that there were more blue QDs than orange in region IV, as compared to more orange than blue QDs in region III. In other words, PL spectra at both regions III and IV provided qualitative evidence of the lateral sieving ability of MWNTs.

Moving into region V, only a single peak at 496.2 ± 0.1 nm (Figure 5V) was formed. This was expected since all orange QDs had been sieved out in region V. In region VI, our final region of investigation, no peak was observed as shown in Figure 5VI. This implied that there were no QDs on the MWNTs sample in this region. To further support the use of MWNTs as a nanosieve, Figure 5b shows a graph of the ratio of area under orange peak (A_O) to area under blue peak (A_B) *vs* distance from the point of reference x, as indicated by the arrow in Figure 5a, with the line connecting the points functioning only as a guide to the eye.

Proposed Mechanism for the Nanosieve. Similarities between our QDs sieving experiment and that of capillary-action chromatography allowed us to propose a working mechanism for the nanosieve. Typical capillary-action chromatography involves dissolving solute in solvent and making use of different attractive forces between the elements to cause different components to spread over different distances. Following similar ideas from capillary-action chromatography while taking note that the particles in our case were suspended and not dissolved in solvent, we propose that the MWNTs served as a nanosieve by trapping larger particles while allowing smaller particles to flow through when the solvent containing the suspended QDs flows through the MWNT network. Figure 6 shows a schematic of the proposed mechanism for the nanosieve. A droplet of blue and orange QDs mixture was deposited onto as-grown MWNTs, and the solvent traveled along and into the MWNT network while undergoing an evaporation process at the same time. The trapping of larger QDs was easier as compared to smaller particles. MWNTs produced *via* our PECVD method show a certain degree of entanglement as observed in Figure 7. Because of the interlacing of MWNT network and the continuous flow of solvent, larger sized particles tend to be trapped nearer to the surface and the region where the droplet was deposited. Smaller particles, unlikely to be trapped, were thus able to travel deeper into and further across the MWNTs. Given the same amount of solvent, larger particles have lower degree of mobility compared to smaller particles. Thus, even if the smaller particles were trapped at the surface, their larger mobility allowed them to escape and spread out. Only when the solvent evaporates, would the smaller QDs be trapped.

Vertical Nanosieve. According to the proposed mechanism above, we anticipate sorting of the QDs mixture to occur in the *z*-direction, that is, in the direction perpendicular to the surface of the sample. To test the hypothesis of a *z*-directional nanosieve, we made use of laser pruning with reduced laser power to trim away the top portion of the mixed QDs-decorated MWNT array.

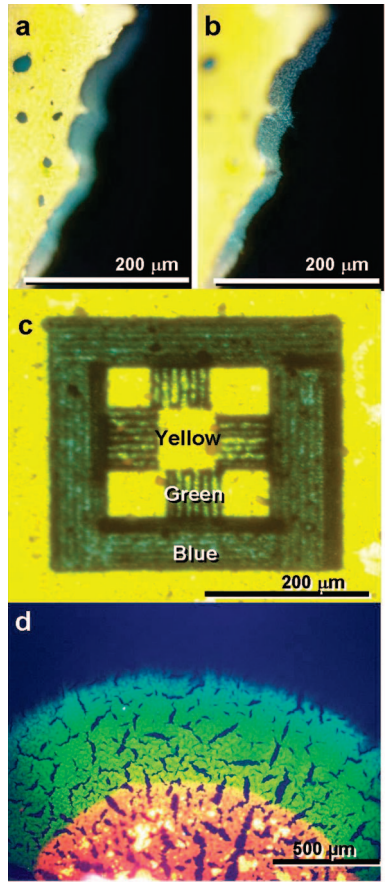

Figure 9. (a−b) FM images of a MWNT sample, decorated with a droplet of QDs mixture, tilted to reveal its side profile: (a) focused on the top orange region of the sample; (b) focused on the collapsed MWNT array showing blue CdSe/ZnS QDs diffused into the MWNT sample; (c) FM image of "blue framed, orange-green checker box" multicolored MWNT pattern created by laser pruning using laser power of ~40 mW (blue) and ~23 mW (green); (d) FM image of MWNT sample decorated with a mixture of QDs consisting of 4.0 nm (orange), 2.6 nm (yellow), and 2.1 nm (green).

This study would reveal any QDs that ventured deeper into the MWNT network. Figure 8a shows a FM image of a patterned sample created using a laser power of ~40 mW with corresponding depth of 7 μm. On an untrimmed surface, a PL peak at 588.4 ± 0.1 nm (Figure 8c) was observed and was responsible for the yellowish orange region seen. On regions pruned by laser, blue light was observed and the PL spectrum showed two peaks at 498.9 ± 0.1 and 599.0 ± 0.1 nm (Figure 8d), respectively. The appearance of a peak at lower wavelength was associated to emission of blue light while the peak at higher wavelength was attributed to saturated yellowish orange visible light around the blue regions. Figure 8b shows a FM image of a patterned sample created similarly using a lower laser power of ~23.0 mW, which slightly trimmed off the top region of the sample to a depth of 1 μm. Creating the same Merlion pattern as shown in Figure 8a, a yellowish green light was emitted from the trimmed region. The PL peak for this region was found to be at 575.3 ± 0.1 nm (Figure 8e), within the yellowish green visible light region. This suggested that the MWNTs were still substantially covered with the larger QDs at this depth within the MWNT array despite a clear reduction in the density of the QDs.

Besides using laser pruning, turning the decorated MWNT sample to its side also revealed the location of the different QDs along the longitudinal axis of the nanotubes. Side view FM and SEM were used to confirm the position of different QDs along the MWNTs. Figure 9 shows a FM image of a decorated MWNT sample tilted to reveal its side profile. From Figure 9a, the top was covered with only orange QDs. Changing the focus, Figure 9b shows that blue QDs had seeped into the MWNT array. The observation was consistent with our proposed mechanism. Thus, the 3D aligned MWNT network served as an effective medium to sieve out QDs with a size difference of ~2.0 nm. Exploiting this effect together with the versatility of the laser pruning technique, one could create patterned microstructures made of MWNTs with different levels of MWNT microstructures exhibiting different colors. With good control of laser power, a multicolored MWNT display was attained as shown in Figure 9c. To identify the limit of the nanosieve, we carried out additional experiments and deposited a drop of solution with three types of QDs onto the MWNT array. The core sizes of the QDs were 4.0, 2.6, and 2.1 nm. Figure 9d shows the FM image of the resultant deposition. From experimental observations, sorting was most effective for particles with larger size difference. Nevertheless, the MWNT array was still efficient in separating particles with size difference as small as 0.5 nm since we were able to identify regions emitting different colors (yellow and green) from the FM image shown.

CONCLUSION

In summary, we have presented two techniques for the assembly of QDs suspended in fast evaporating solvents such as chloroform and toluene onto MWNT templates created by laser pruning technique. Post assembly laser patterning was adopted to bypass the problem of cellular pattern formation in MWNTs during the droplet-drying deposition method. Through assembly of a mixture of QDs with ~2.0 nm size difference onto MWNTs, followed by careful tuning of laser power, multicolored display of QDs on MWNTs were created. Evidences exhibiting the ability of aligned MWNTs to serve as a 3D filter that can physically sort out particles with mere size differences of ~0.5 nm were also obtained. These experiments illustrated a 3D nanosieve that exhibits size-preferential trapping of the nanoparticles by the MWNT network. We believe that such selective and controlled assemblies of QDs on MWNTs could be used as multifunctional components of hybrid material system. With careful laser power tuning, a multicolor display could also be created.

METHODS

MWNTs and Laser Pruning. Aligned multiwalled CNTs (MWNTs) with a typical length of 30−40 μm were grown on clean N-typed silicon (3 mm × 5 mm, (100) Si) substrates containing native oxide layer. Before growth, a layer of iron film was coated on the substrates as catalyst using a magnetron sputtering system (model RF Magnetron Denton Discovery 18). The coating rate was 4 nm/min lasting for 3.25 min. These MWNTs were synthesized using a plasma enhanced chemical vapor deposition (PECVD), and details of the growth process were reported elsewhere.[24–26] With laser pruning technique,[23] channels and patterns were created on the MWNT films. By adjusting the laser power, we were able to create MWNT structures of various height and thus create 3D microstructures.

Quantum Dots. Cadmium selenide (CdSe) core shell quantum dots coated with zinc sulfide (ZnS) capping (CdSe/ZnS QDs) of various sizes and hence emission colors were purchased from Evident Technologies. The sizes of QDs used include 1.9 nm (blue), 2.1 nm (green), 2.6 nm (yellow), and 4.0 nm (orange). These QDs came in respective concentrations of 150, 132.0, 41.0, and 20.7 nmol/ml. Their individual emission peaks were 490, 520.0, 560.0, and 600.0 nm. Their outer shells were covered with a 16 hydrocarbon ligand. The ZnS capping helped to prevent the quenching effect of uncoordinated atoms[27] on the surfaces of CdSe nanocrystals and hence enhanced the photoluminescence (PL) property.[28] All sizes of the QDs mentioned in this report corresponded to the diameter of the CdSe core and the ZnS shell was a few monolayers in thickness. These commercially purchased QDs were suspended in either chloroform or toluene, which were found to spread across MWNTs rapidly.

Further Characterizations. Further characterizations of the samples were carried out using a scanning electron microscope (SEM, JEOL JSM-6400F), transmission electron microscope (TEM, JEOL JEM-2010F), fluorescence microscope (FM, Olympus IX71S1F-3 Inverted Microscope) and photoluminescence microscope (PLM, Rashaw 5161R-G with a Kimmon 1K Series He−Cd Laser).

Acknowledgment. We thank the generous support of an ASTAR TSRP PMED grant.

Supporting Information Available: Comparison between outcomes of patterns pruned on MWNTs using method 1 and method 2. This material is available free of charge *via* the Internet at http://pubs.acs.org.

REFERENCES AND NOTES

1. Iijima, S. Helical Microtubules of Graphitic Carbon. *Nature* **1991**, *354*, 56–58.
2. Ajayan, P. M.; Zhou, O. Z. Carbon Nanotubes: Synthesis, Structure, Properties and Applications. In *Topics in Applied Physics*; Dresselhaus M. S., Dresselhaus, G., Avouris, P., Eds.; Springer-Verlag: Berlin, Heidelberg, 2001; Vol. 80, pp 391−425.
3. Wilder, J. W. G.; Venema, L. C.; Rinzler, A. G.; Smalley, R. E.; Dekker, C. Electronic Structure of Atomically Resolved Carbon Nanotubes. *Nature* **1998**, *391*, 59–62.
4. Treacy, M. M. J.; Ebbesen, T. W.; Gibson, J. M. Exceptionally High Young's Modulus Observed for Individual Carbon Nanotubes. *Nature* **1996**, *381*, 678–680.
5. Jang, J. W.; Lee, D. K.; Lee, C. E.; Lee, T. J.; Lee, C. J.; Noh, S. J. Metallic Conductivity in Bamboo-Shaped Multiwalled Carbon Nanotubes. *Solid State Commun.* **2002**, *122*, 619–622.
6. Tekleab, D.; Czerw, R.; Carroll, D. L.; Ajayan, P. M. Electronic Structure of Kinked Multiwalled Carbon Nanotubes. *Appl. Phys. Lett.* **2000**, *76*, 3594–3596.
7. Olek, M.; Bšgen, T.; Hilgendorff, M.; Giersig, M. Quantum Dot Modified Multiwall Carbon Nanotubes. *J. Phys. Chem. B.* **2006**, *110*, 12901–12904.
8. Haremza, J. M.; Hahn, M. A.; Chen, S.; Calcines, J.; Krauss, T. D. Attachment of Single CdSe Nanocrystals to Individual Single-Walled Carbon Nanotubes. *Nano Lett.* **2002**, *2*, 1253–1258.
9. Huang, W. J.; Taylor, S.; Fu, K. F.; Lin, Y.; Zhang, D. H.; Hanks, T. W.; Rao, A. M.; Sun, Y. P. Attaching Proteins to Carbon Nanotubes *via* Diimide-Activated Amidation. *Nano Lett.* **2002**, *2*, 311–314.
10. Pompeo, F.; Resasco, D. E. Water Solubilization of Single-Walled Carbon Nanotubes by Functionalizations with Glucosamine. *Nano Lett.* **2002**, *2*, 369–373.
11. Correa-duarte, M. A.; Wagner, N.; Rojas-Chapana, J.; Morsczeck, C.; Thie, M.; Giersig, M. Fabrication and Biocompatibility of Carbon Nanotube-Based 3D Networks as Scaffolds for Cell Seeding and Growth. *Nano Lett.* **2004**, *4*, 2233–2236.
12. Zhu, Y. W.; Elim, H. I.; Foo, Y. L.; Yu, T.; Liu, Y.; Ji, W.; Lee, J.; Shen, Z.; Wee, A. T. S.; Thong, J. T. L.; *et al.* Multiwalled Carbon Nanotubes Beaded with ZnO Nanoparticles for Ultrafast Nonlinear Optical Switching. *Adv. Mater.* **2006**, *18*, 587–592.
13. Rocha, C. G.; Dargam, T. G.; Latgé, A. Electronic States in Zigzag Carbon Nanotubes Quantum Dots. *Phys. Rev. B* **2002**, *65*, 165431-1–165431-7.
14. Alivisatos, A. P. Perspectives on the Physical Chemistry of Semiconductor Nanocrystals. *J. Phys. Chem.* **1996**, *100*, 13226–13239.
15. Robel, I.; Bunker, B. A.; Kamat, P. V. Single-Walled Carbon Nanotube-CdS Nanocomposites as Light-Harvesting Assemblies: Photoinduced Charge-Transfer Interactions. *Adv. Mater.* **2005**, *17*, 2458–2463.
16. Gust, A.; Kruse, C.; Hommel, D. Investigation of CdSe Quantum Dots in MgS Barriers as Active Region in Light Emitting Diodes. *J. Cryst. Growth* **2007**, *301−302*, 789–792.
17. Banerjee, S.; Wong, S. S. Synthesis and Characterization of Carbon Nanotube-Nanocrystal Heterostructures. *Nano Lett.* **2002**, *2*, 195–200.
18. Haremza, J. M.; Hahn, M. A.; Krauss, T. D. Attachment of Single CdSe Nanocrystals to Individual Single-Walled Carbon Nanotubes. *Nano Lett.* **2002**, *2*, 1253–1258.
19. Chan, W. C. W.; Nie, S. Quantum Dot Bioconjugates for Ultrasensitive Nonisotopic Detection. *Science (Washington, D. C.)* **1998**, *281*, 2016–2018.
20. Ravindran, S.; Bozhilov, K. N.; Ozkan, C. S. Self Assembly of Ordered Artificial Solids of Semiconducting ZnS Capped CdSe Nanoparticles at Carbon Nanotube Ends. *Carbon* **2004**, *42*, 1537–1542.
21. Grzelczak, M.; Correa-Duarte, M. A.; Salgueiriño-Maceira, V.; Giersig, M.; Diaz, R.; Liz-Marzán, L. M. Photoluminescence Quenching Control in Quantum Dot-Carbon Nanotube Composite Colloids Using a Silica-Shell Spacer. *Adv. Mater.* **2006**, *18*, 415–420.
22. Chakrapani, N.; Wei, B.; Carrillo, A.; Ajayan, P. M.; Kane, R. S. From the Cover: Capillarity-Driven Assembly of Two-Dimensional Cellular Carbon Nanotube Foams. *Proc. Natl. Acad. Sci. U.S.A.* **2004**, *101*, 4009–4012.
23. Lim, K. Y.; Sow, C. H.; Lin, J.; Cheong, F. C.; Shen, Z. X.; Thong, J. T. L.; Chin, K. C.; Wee, A. T. Saser Pruning of Carbon Nanotubes as a Route to Static and Movable Structures. *Adv. Mater.* **2003**, *15*, 300–303.
24. Zhu, Y. W.; Cheong, F. C.; Yu, T.; Xu, X. J.; Lim, C. T.; Thong, J. T. L.; Shen, Z. X.; Ong, C. K.; Liu, Y. J.; Wee, A. T. S.; *et al.* Effects of CF_4 Plasma on the Field Emission Properties of Aligned Multi-Wall Carbon Nanotube Films. *Carbon* **2005**, *43*, 395–400.
25. Wang, Y. H.; Lin, J.; Huan, C. H. A.; Chen, G. S. Synthesis of Large Area Aligned Carbon Nanotubes Arrays from C_2H_2-H_2 Mixture by RF Plasma-Enhanced Chemical Vapor Deposition. *Appl. Phys. Lett.* **2001**, *79*, 680–682.
26. Bell, M. S.; Teo, K. B. K.; Lacerda, R. G.; Milne, W. I.; Hash, D. B.; Meyyappan, M. Carbon Nanotubes by Plasma-Enhanced Chemical Vapor Deposition. *Pure Appl. Chem.* **2006**, *78*, 1117–1125.
27. Myung, N.; Ding, Z.; Bard, A. J. Electrogenerated Chemiluminescence of CdSe Nanocrystals. *Nano Lett.* **2002**, *2*, 1315–1319.
28. Schlamp, M. C.; Pang, X.; Alivisatos, A. P. Improved Efficiencies in Light Emitting Diodes Made with CdSe(CdS) Core/Shell Type Nanocrystals and a Semiconducting Polymer. *J. Appl. Phys.* **1997**, *82*, 5837–5842.